

Characteristics of Density and Temperature Fluctuation in Fusion Edge Plasma and Implication on Scrape off Layer Width

Shimpei ARAI and Yusuke KOSUGA¹⁾

Interdisciplinary Graduate School of Engineering Sciences, Kyushu University, Kasuga, Fukuoka 816-8580, Japan

¹⁾*Research Institute for Applied Mechanics, Kyushu University, Kasuga 816-8580, Japan*

(Received 16 February 2022 / Accepted 28 March 2022)

In this study, in order to evaluate the SOL width of both density and temperature, we analyze Hasegawa-Wakatani model which includes the temperature fluctuations. Different instability regimes, i.e. drift waves and linearly unstable convective cells are studied. It is shown that convective cells are favorable in terms of the heat load reduction on the divertor. Implications on future devices, such as JT-60 SA, ITER, etc, are discussed.

© 2022 The Japan Society of Plasma Science and Nuclear Fusion Research

Keywords: SOL, turbulence, instability, drift wave, convective cell, adiabatic electron, hydrodynamic electron

DOI: 10.1585/pfr.17.1403050

1. Introduction

Divertor heat load is a major concern for a fusion reactor. In ITER, it is estimated that the heat flux passing through Scrape off Layer (SOL) reaches 1 [GW/m²] in the parallel direction and 50 ~ 100 [MW/m²] in the perpendicular direction [1]. This value can be even higher for the prototype reactor. Since these values exceed the limit required from the engineering constraint, i.e. 10 ~ 20 [MW/m²], it is a critical issue to understand the physical mechanism behind the divertor heat load and to develop a scenario for the heat load reduction [2]. The heat flux of SOL is characterized by $q_{sol} = P/(2\pi R\lambda_{sol})$ [3], where P is power from the core plasma, R is a major radius, and λ_{sol} is a SOL width. Then the SOL width is a key parameter in evaluating the heat flux on the divertor [4]. A heuristic model has been derived based on ∇B drift [5]. While the prediction was rather pessimistic, the role of fluctuations was overlooked. Indeed, several studies indicate the importance of turbulence transport to widen the SOL width [6]. These studies addressed the impact of drift waves [4], parallel velocity gradient driven modes [7,8], interchange modes [9], streamers [10], blobs [11,12], etc.

At the simplest level, turbulence increases transport and appears to be beneficial to widen the SOL width. On the other hand, it is also well known that turbulent transport exhibits various interference [13]. Namely, the flux down the gradient co-exists with the flux up the gradient. Typical example of this is the various up-gradient phenomena in heat driven tokamaks. For example, while the heat flux is down the temperature gradient in fusion plasmas, this heat flux drives various up gradient phenomena, such as particle pinch [14], excitation of zonal flows and intrinsic rotation [15], etc. Particle pinch by PVG turbulence is also reported [16,17]. In the context of the SOL width,

these up-gradient or inward fluxes are undesirable, since they can narrow the width. In this sense, care must be taken to address the role of turbulence on widening SOL width. In particular, it is desirable to identify the fluctuations that can drive the flux down the gradient, both in heat and particles.

The aim of this study is to describe the typical feature of edge fluctuations in fusion plasmas and summarize their role in driving transport in different channels. To be specific, we focus on the particle and heat transport, as they have more direct impact on divertor heat load. To demonstrate the subtlety of the coupled transport, we start by analyzing typical edge fluctuations, i.e. collisional drift waves. We introduce an extended Hasegawa-Wakatani model [18], which incorporate both density and electron temperature fluctuation dynamics. The extended model is used to discuss that the two different fluctuations are excited. When the electron response is close to adiabatic, drift waves are excited. In this regime, the particle flux is outward. Here the direction ‘outward’ denotes the direction away from the core. Likewise, inward is for the direction toward the core. The heat flux is sensitive to the ratio between electron temperature gradient and the density gradient η_e , and in some cases the heat flux can be inward. There is another regime of interest for fluctuations. This is when the electron motion is limited to the direction perpendicular to the magnetic field. In this case, the fluctuation looks rather different from drift waves and the density and temperature responses become larger. We call this regime as linearly unstable drift convective cells and they drive outward flux both for particles and heat, which is favorable for the SOL width control. The condition for convective cell excitation is discussed using parameters from several experiments.

The remainder of the paper is organized as follows. In the Sec. 2, we describe the model used in this work. Here the extension of the Hasegawa-Wakatani model to include

author's e-mail: kosuga@riam.kyushu-u.ac.jp

the electron temperature is discussed. Section 3 describes the relevant feature of drift waves. Their impact on the density and temperature perturbations is summarized. In Sec. 4, we discuss the excitation of convective cells and their impact on transport. Section 5 presents the parameter survey for different experiments and summarizes the implication on future larger devices. Section 6 is conclusion.

2. Model

In this work we are interested in the fluctuation dynamics in the edge-SOL region of fusion plasmas. To model its dynamics, we use Hasegawa-Wakatani (HW) model [18]. The HW equation is based on the evolution of two fields, density and vorticity. In order to elucidate the complexity of the transport process in the edge region, we use extended HW model with electron temperature evolution. The electron fluctuation can be incorporated into the HW model from the Braginskii equation [19, 20]. The electron temperature evolution is given by

$$\frac{3}{2}n_e \frac{dT_e}{dt} + n_e T_e \nabla_{\parallel} v_{e\parallel} - n_e \chi_{\parallel} \nabla_{\parallel}^2 T_e - \frac{\alpha_T T_e}{e} \nabla_{\parallel} J_{\parallel} = 0, \quad (1)$$

$$\frac{d}{dt} = \partial_t + v_{e\parallel} \nabla_{\parallel} + \mathbf{v}_{E \times B} \cdot \nabla. \quad (2)$$

Here, \parallel is the direction for the mean magnetic field. In the perpendicular direction to the field, we use (x, y) , which corresponds to (r, θ) . n_e is the electron density, e is the electron charge, T_e is the electron temperature, $\chi_{\parallel} = 3.16 v_{the}^2 / \nu_e$ is the parallel thermal diffusivity. α_T is a dimensionless number which depends on the charge number Z . For hydrogens, we have $Z = 1$ and $\alpha_T = 0.71$ [19, 20]. The temperature evolution is determined by the compression of the electron fluids, conduction, and the heat generation associated with the thermal force. The electron temperature field then introduces a new force, the thermal force on electrons. The parallel momentum balance for electrons reads as

$$0 = -\nabla_{\parallel} p_e - en_e E_{\parallel} - m_e n_e \nu_e v_{e\parallel} - \alpha_T n_e \nabla_{\parallel} T_e. \quad (3)$$

Here m_e is the electron mass, $\nu_e = 2.91 \times 10^{-6} n_e / T_e^{-\frac{3}{2}} \ln \Lambda$ is the electron collision frequency. The lefthand side is set to zero because the electron mass is small. The righthand side includes several forces, such as the parallel pressure gradient, the parallel electric field, the collisional drag on the electron, and the thermal force. Using the $p_e = n_e T_e$ and assuming electrostatic fluctuations, fluctuating parallel electron velocity is given as

$$\tilde{v}_{e\parallel} = D_{\parallel} \nabla_{\parallel} \left(\frac{\tilde{n}}{n_0} - \frac{e\tilde{\phi}}{T_{e0}} + (1 + \alpha_T) \frac{\tilde{T}_e}{T_{e0}} \right). \quad (4)$$

Here ϕ is the electrostatic potential, $D_{\parallel} = v_{the}^2 / \nu_e$ is the parallel electrons diffusivity, and $v_{the} = \sqrt{T_e / m_e}$ is the electron thermal velocity. Fluctuating component is denoted by

$(\tilde{\cdot})$, and the subscript $(\dots)_0$ is for the background component. The temperature evolution and the parallel electron velocity fluctuations are coupled together with the electron density evolution and the charge neutrality condition $\nabla \cdot \mathbf{J} = 0$, to obtain the Hasegawa-Wakatani model with temperature evolution as

$$\frac{d \tilde{n}_e}{dt n_0} + v_{*e} \frac{\partial}{\partial y} \frac{e\tilde{\phi}}{T_{e0}} = D_{\parallel} \nabla_{\parallel}^2 \left(\frac{\tilde{n}_e}{n_0} - \frac{e\tilde{\phi}}{T_{e0}} + (1 + \alpha_T) \frac{\tilde{T}_e}{T_{e0}} \right), \quad (5)$$

$$\frac{d}{dt} \rho_s^2 \nabla_{\perp}^2 \frac{e\tilde{\phi}}{T_{e0}} = D_{\parallel} \nabla_{\parallel}^2 \left(\frac{\tilde{n}_e}{n_0} - \frac{e\tilde{\phi}}{T_{e0}} + (1 + \alpha_T) \frac{\tilde{T}_e}{T_{e0}} \right), \quad (6)$$

$$\frac{3}{2} \frac{d \tilde{T}_e}{dt T_{e0}} + \frac{3}{2} \eta_e v_{*e} \frac{\partial}{\partial y} \frac{e\tilde{\phi}}{T_{e0}} - \chi_{\parallel} \nabla_{\parallel}^2 \frac{\tilde{T}_e}{T_{e0}} = (1 + \alpha_T) D_{\parallel} \nabla_{\parallel}^2 \left(\frac{\tilde{n}_e}{n_0} - \frac{e\tilde{\phi}}{T_{e0}} + (1 + \alpha_T) \frac{\tilde{T}_e}{T_{e0}} \right). \quad (7)$$

Here, ρ_s is the ion sound larmor radius, $v_{*e} = (\rho_s / L_n) c_s$ is the drift velocity, L_n is the density gradient length, L_T is the temperature gradient length, $\eta_e = L_n / L_T$. Not surprisingly, the HW model is recovered by ignoring the terms related to the temperature fluctuation in Eqs. (5) and (6). Hereafter we use the normalized quantities, denoted by $\tilde{n}_e / n_0 \rightarrow \hat{n}$, $e\tilde{\phi} / T_{e0} \rightarrow \hat{\phi}$, $\tilde{T}_e / T_{e0} \rightarrow \hat{T}$.

Fluctuation properties are analyzed by linear analysis. Linearizing ($d/dt \rightarrow \partial/\partial t$) and Fourier transforming ($\partial/\partial t \rightarrow -i\omega$, $\nabla \rightarrow i\mathbf{k}$), Eqs. (5) - (7) become as

$$-i\omega \hat{n} + i\omega_{*e} \hat{\phi} = -D_{\parallel} k_{\parallel}^2 (\hat{n} - \hat{\phi} + (1 + \alpha_T) \hat{T}), \quad (8)$$

$$i\omega \rho_s^2 k_{\perp}^2 \hat{\phi} = -D_{\parallel} k_{\parallel}^2 (\hat{n} - \hat{\phi} + (1 + \alpha_T) \hat{T}), \quad (9)$$

$$-\frac{3}{2} i\omega \hat{T} + \frac{3}{2} i\eta_e \omega_{*e} \hat{\phi} = -D_{\parallel} k_{\parallel}^2 (\hat{n} - \hat{\phi} + (1 + \alpha_T) \hat{T}) - \chi_{\parallel} k_{\parallel}^2 \hat{T}. \quad (10)$$

Here, $\omega_{*e} = k_y \rho_s (c_s / L_n)$ is the electron drift frequency. The density and temperature responses are obtained as

$$\hat{n} = \frac{\omega_{*e}}{\omega} \hat{\phi} - \rho_s^2 k_{\perp}^2 \hat{\phi}, \quad (11)$$

$$\hat{T} = \frac{(1 + \alpha_T)}{-3i\omega/2 + \chi_{\parallel} k_{\parallel}^2} \left[-\frac{3}{2} \frac{\eta_e i\omega_{*e}}{1 + \alpha_T} + i\omega \rho_s^2 k_{\perp}^2 \right] \hat{\phi}. \quad (12)$$

The dispersion relation is obtained by substituting the density and temperature perturbation into the quasi-neutrality, i.e. the vorticity evolution (Eq. (9)). The result is

$$-\frac{i\omega \rho_s^2 k_{\perp}^2}{D_{\parallel} k_{\parallel}^2} = \frac{\omega_{*e}}{\omega} - 1 - \rho_s^2 k_{\perp}^2 + \frac{(1 + \alpha_T)^2}{-3i\omega/2 + \chi_{\parallel} k_{\parallel}^2} \left[-\frac{3}{2} \frac{\eta_e i\omega_{*e}}{1 + \alpha_T} + i\omega \rho_s^2 k_{\perp}^2 \right]. \quad (13)$$

The dispersion relation can be simplified in several relevant limits. To address this, we note that there are two characteristic time scales in the model (Fig. 1). One is for

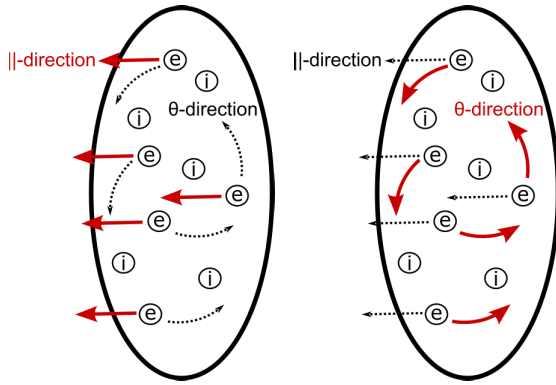


Fig. 1 Electron response. (a) is for $D_{\parallel}k_{\parallel}^2 \gg \omega_{*e}$ and (b) is for $\omega_{*e} \gg D_{\parallel}k_{\parallel}^2$.

the diffusion along the magnetic field, which is given by $k_{\parallel}^2 D_{\parallel} \sim k_{\parallel}^2 \chi_{\parallel}$. The other is the drift frequency, ω_{*e} . Using these two time scales, we can discuss different regimes of the fluctuations. For example, when $D_{\parallel}k_{\parallel}^2 \gg \omega_{*e}$, electrons diffuse rapidly along the magnetic field. Electron response is expected to be close to the Boltzmann response. On the other hand, when $\omega_{*e} \gg D_{\parallel}k_{\parallel}^2$, electrons drift poloidally before they travel along the magnetic field. Electron motion is expected to be confined to the perpendicular plane and fluctuation characteristics deviates from that with the adiabatic electron response. The latter regime is called hydrodynamic [21]. Both limits are considered separately in the following and we discuss the relevant fluctuation characteristics, including dispersion relation, amplitude and phase relation, and transport feature.

3. Adiabatic Electrons: Drift Wave

We first discuss the adiabatic limit, $D_{\parallel}k_{\parallel}^2 \gg \omega_{*e}$. In this case, the electron response is close to the Boltzmann response. Drift waves are excited and transport interference may occur, as discussed in the following. In this section, we introduce a small parameter by $\omega_{*e}/(k_{\parallel}^2 D_{\parallel})$ to perform perturbative expansion. Simplified dispersion relation, fluctuation characteristics, quasilinear transport flux, are obtained in the limit of $\omega_{*e}/(k_{\parallel}^2 D_{\parallel}) \ll 1$.

3.1 Dispersion relation

The generalized dispersion relation (Eq. (13)) can be simplified by taking the limit $\omega \sim \omega_{*e} \ll k_{\parallel}^2 D_{\parallel}$. Writing $\omega = \omega^{(0)} + \delta\omega$, where $\omega^{(0)}$ is the lowest order solution and $\delta\omega/\omega^{(0)} \sim O(\omega_{*e}/k_{\parallel}^2 D_{\parallel})$, Eq. (13) becomes

$$-i \frac{(\omega^{(0)} + \delta\omega) \rho_s^2 k_{\perp}^2}{D_{\parallel} k_{\parallel}^2} = \frac{\omega_{*e}}{(\omega^{(0)} + \delta\omega)} - 1 - \rho_s^2 k_{\perp}^2 + \frac{(1 + \alpha_T)^2}{\chi_{\parallel} k_{\parallel}^2} \left[-\frac{3}{2} \frac{\eta_e i \omega_{*e}}{1 + \alpha_T} + i(\omega^{(0)} + \delta\omega) \rho_s^2 k_{\perp}^2 \right]. \quad (14)$$

Collecting the lowest order contribution, we have

$$0 \simeq \frac{\omega_{*e}}{\omega^{(0)}} - 1 - \rho_s^2 k_{\perp}^2,$$

and therefore

$$\omega^{(0)} = \frac{\omega_{*e}}{1 + \rho_s^2 k_{\perp}^2}. \quad (15)$$

Thus the typical fluctuation of interest in this regime is drift wave.

The next order contribution is evaluated as:

$$-i \frac{\omega^{(0)} \rho_s^2 k_{\perp}^2}{D_{\parallel} k_{\parallel}^2} \simeq -\frac{\omega_{*e} \delta\omega}{\omega^{(0)2}} + i \frac{(1 + \alpha_T)^2}{\chi_{\parallel} k_{\parallel}^2} \left[\omega^{(0)} \rho_s^2 k_{\perp}^2 - \frac{3}{2} \frac{\eta_e \omega_{*e}}{1 + \alpha_T} \right],$$

and therefore

$$\delta\omega = i \frac{\omega^{(0)2}}{\omega_{*e}} \delta_n, \quad (16)$$

$$\delta_n = \frac{\omega_{*e}}{D_{\parallel} k_{\parallel}^2} \frac{\rho_s^2 k_{\perp}^2}{1 + \rho_s^2 k_{\perp}^2} + \frac{(1 + \alpha_T)^2 \omega_{*e}}{\chi_{\parallel} k_{\parallel}^2} \frac{\rho_s^2 k_{\perp}^2}{1 + \rho_s^2 k_{\perp}^2} - \frac{3}{2} (1 + \alpha_T) \frac{\eta_e \omega_{*e}}{\chi_{\parallel} k_{\parallel}^2}. \quad (17)$$

The growth rate is given by $\gamma = \text{Im}(\omega) = \delta_n(\omega^{(0)2}/\omega_{*e})$. For drift waves to be unstable, we must have $\delta_n > 0$. The density gradient destabilizes drift waves, and dissipation is required for instability. Here the dissipation is due to collisions associated with the parallel motion. The temperature gradient is stabilizing for collisional drift waves.

3.2 Amplitude and phase

More fluctuation characteristics can be obtained by analyzing the relative amplitude and phase relation between fluctuations. By using the obtained dispersion relation, the density perturbation Eq. (11) now becomes

$$\hat{n} = (1 - i\delta_n) \hat{\phi}. \quad (18)$$

The density response is close to the Boltzmann response, $\hat{n} \sim \hat{\phi}$. A finite phase shift exist between the density and potential perturbation. The phase shift is required for the mode to be unstable. These are well-known properties of collisional drift waves.

The temperature response can be simplified in the similar manner. The result is

$$\hat{T} = i \frac{(1 + \alpha_T) \omega_{*e}}{\chi_{\parallel} k_{\parallel}^2} \left[\frac{\rho_s^2 k_{\perp}^2}{1 + \rho_s^2 k_{\perp}^2} - \frac{3}{2} \frac{\eta_e}{1 + \alpha_T} \right] \hat{\phi}. \quad (19)$$

Unlike the density response, the temperature response is smaller compared to the potential and the density, $\hat{T} \ll \hat{\phi} \sim \hat{n}$. The phase relation has interesting feature. First of all, the phase is shifted by $\pi/2$. Whether it is retarded or advanced depends on the relative sign in the parenthesis. Namely, $\hat{T} \sim e^{-i\pi/2}$ for $\frac{\rho_s^2 k_{\perp}^2}{1 + \rho_s^2 k_{\perp}^2} - \frac{3}{2} \frac{\eta_e}{1 + \alpha_T} < 0$, while $\hat{T} \sim e^{i\pi/2}$ for $\frac{\rho_s^2 k_{\perp}^2}{1 + \rho_s^2 k_{\perp}^2} - \frac{3}{2} \frac{\eta_e}{1 + \alpha_T} > 0$. This competition is due to the

fact that there are two distinct source for the temperature perturbation. One is fluctuation associated with the gradient η_e and the other is fluctuation associated with compression/divergence, $\nabla_{\parallel} v_{e\parallel}$. The competition between the two process determines whether the temperature perturbation is retarded or advanced relative to the density and potential perturbations [22].

3.3 Flux

The flux driven by drift waves can be analyzed by the quasilinear theory. The particle flux is given as

$$\frac{\Gamma_n}{n_0 c_s} = \rho_s \left\langle \hat{n} \left(-\frac{\partial}{\partial y} \hat{\phi} \right) \right\rangle = \sum_k \rho_s k_y \delta_n |\phi_k|^2. \quad (20)$$

The particle flux is positive for unstable drift waves and drift waves relax the density profile. The flux is proportional to the phase shift. We also note that for a given level of potential fluctuations, the particle flux is in the order of $O(\omega_{*e}/k_{\parallel}^2 D_{\parallel})$.

The heat flux is also obtained as

$$\begin{aligned} \frac{Q_e}{T_e c_s} &= \rho_s \left\langle \hat{T} \left(-\frac{\partial}{\partial y} \hat{\phi} \right) \right\rangle \\ &= - \sum_k \rho_s k_y \frac{(1 + \alpha_T) \omega_{*e}}{\chi_{\parallel} k_{\parallel}^2} \left[\frac{\rho_s^2 k_{\perp}^2}{1 + \rho_s^2 k_{\perp}^2} - \frac{3}{2} \frac{\eta_e}{1 + \alpha_T} \right] |\phi_k|^2. \end{aligned} \quad (21)$$

The normalized amplitude is in the order of $Q_e \sim O(\omega_{*e}/k_{\parallel}^2 \chi_{\parallel})$ and its magnitude is close to that of the particle flux. The sign depends on the sign of the phase, or the relative sign between the compression and the gradient driven terms. $Q_e > 0$ when ∇T_e dominates in the temperature response, while $Q_e < 0$ when compression dominates in the temperature response.

4. Hydrodynamic Electrons: Linearly Unstable Convective Cell

Here we consider the case with $\omega_{*e} \gg k_{\parallel}^2 D_{\parallel}$. The coupling along the magnetic field becomes weaker and the electron motion is close to the 2D motion in the perpendicular plane, as depicted in Fig. 1. Fluctuation characteristics is very different from that of drift waves, as shown in the following. In this section, we consider the opposite limit from the previous section, and the expansion parameter is $k_{\parallel}^2 D_{\parallel} / \omega_{*e} \ll 1$. Since this limit corresponds to the small k_{\parallel} and the evolution of the vortex is close to the 2D vortex, we refer the mode excited here to convective cells. We note that the word of the convective cells is often used to describe the 2D vortex driven nonlinearly. Here we use this word in a broader sense, regardless of the driving force. As shown below, small, but finite k_{\parallel} coupling allows convective cells to access to the free energy in the density gradient. This leads to the excitation of linearly unstable convective cells, which we call as drift convective cells.

4.1 Dispersion relation

In order to elucidate the typical time scale in this limit, we consider the simplified system of the equations. To do so, we consider the usual HW model without the coupling to temperature fluctuation. In this case, the generalized dispersion relation reduces to

$$-\frac{i \omega \rho_s^2 k_{\perp}^2}{D_{\parallel} k_{\parallel}^2} = \frac{\omega_{*e}}{\omega} - 1 - \rho_s^2 k_{\perp}^2. \quad (22)$$

This can be solved as

$$\omega = \frac{k_{\parallel}^2 D_{\parallel}}{2i \rho_s^2 k_{\perp}^2} \left(1 + \rho_s^2 k_{\perp}^2 \pm \sqrt{(1 + \rho_s^2 k_{\perp}^2)^2 - 4i \frac{\rho_s^2 k_{\perp}^2}{D_{\parallel} k_{\parallel}^2} \omega_{*e}} \right). \quad (23)$$

Taking $\omega_{*e} \gg k_{\parallel}^2 D_{\parallel}$, the dispersion relation reduces to

$$\omega \simeq \frac{\sqrt{D_{\parallel} k_{\parallel}^2 |\omega_{*e}|}}{\rho_s k_{\perp}} \left(\pm \frac{\text{sgn}(k_y) + i}{\sqrt{2}} \right). \quad (24)$$

Here, $\text{sgn}(k_y)$ is

$$\text{sgn}(k_y) = \begin{cases} 1 & k_y > 0 \\ 0 & k_y = 0 \\ -1 & k_y < 0. \end{cases}$$

This simplified analysis identifies the relevant time scale for the frequency ω as $\sqrt{D_{\parallel} k_{\parallel}^2 |\omega_{*e}|}$. Then normalizing the frequency as $\omega = \sqrt{D_{\parallel} k_{\parallel}^2 |\omega_{*e}|} \Omega$, Eq. (13) becomes

$$\begin{aligned} &\frac{i \rho_s^2 k_{\perp}^2}{-D_{\parallel} k_{\parallel}^2} \sqrt{D_{\parallel} k_{\parallel}^2 |\omega_{*e}|} \Omega \\ &= \frac{\omega_{*e}}{\sqrt{D_{\parallel} k_{\parallel}^2 |\omega_{*e}|} \Omega} - 1 - \rho_s^2 k_{\perp}^2 + \frac{(1 + \alpha_T)^2}{-\frac{3}{2} i \sqrt{D_{\parallel} k_{\parallel}^2 |\omega_{*e}|} \Omega} \\ &\left[-\frac{3}{2} \frac{\eta_e i \omega_{*e}}{1 + \alpha_T} + i \rho_s^2 k_{\perp}^2 \sqrt{D_{\parallel} k_{\parallel}^2 |\omega_{*e}|} \Omega \right]. \end{aligned} \quad (25)$$

The lowest order balance is then given by

$$i \rho_s^2 k_{\perp}^2 \sqrt{\frac{|\omega_{*e}|}{D_{\parallel} k_{\parallel}^2}} \Omega \simeq \frac{1}{\Omega} \sqrt{\frac{|\omega_{*e}|}{D_{\parallel} k_{\parallel}^2}} (1 + (1 + \alpha_T) \eta_e) \text{sgn}(k_y),$$

which yields

$$\Omega = \frac{\text{sgn}(k_y) + i}{\sqrt{2}} \frac{\sqrt{1 + (1 + \alpha_T) \eta_e}}{\rho_s k_{\perp}},$$

and

$$\omega = \sqrt{D_{\parallel} k_{\parallel}^2 |\omega_{*e}|} \frac{\text{sgn}(k_y) + i}{\sqrt{2}} \frac{\sqrt{1 + (1 + \alpha_T) \eta_e}}{\rho_s k_{\perp}}. \quad (26)$$

We note that the mode of interest is one realization of the family of convective cells, which can be excited by various processes. Loosely speaking, the evolution of convective cells is analyzed by the vorticity evolution, $\partial \nabla_{\perp}^2 \phi / \partial t$.

There are various sources for the excitation, such as centrifugal force (Rayleigh-Taylor instability), vorticity gradient (Kelvin-Helmholtz instability), nonlinear Reynolds stress (zonal flow/streamers [23,24].), etc. Here, the small, but finite k_{\parallel} allows the coupling between the vorticity field, the density and temperature perturbations. In our case, the coupling allows the cells to access to the free energy in the density and temperature gradient. We call this mode as a drift convective cell. Drift convective cell has very slow frequency, ($\omega_{*e} \gg \omega \gg D_{\parallel}k_{\parallel}^2$). The instability is strong, in the sense that $\text{Re}(\omega) \sim \text{Im}(\omega)$. Namely, the mode grows significantly before it oscillates. This feature may be contrasted to drift waves, which have $\text{Re}(\omega) \gg \text{Im}(\omega)$. Note that once excited, drift convective cells enter the nonlinear stage. Once the nonlinear effect is considered, we can have additional ingredient for the excitation of the cells. The analysis of the nonlinear dynamics of drift convective cells is beyond the scope of the present work and will be pursued in future.

4.2 Amplitude and phase

Drift convective cells have unique feature in the density and temperature response. This point can be clarified by calculating the density and temperature perturbation as

$$\hat{n} = \frac{\rho_s k_{\perp}}{\sqrt{1 + (1 + \alpha_T)\eta_e}} \sqrt{\frac{|\omega_{*e}|}{D_{\parallel}k_{\parallel}^2}} \frac{1 - \text{sgn}(k_y)i}{\sqrt{2}} \hat{\phi}, \quad (27)$$

$$\hat{T} = \rho_s k_{\perp} \sqrt{\frac{\eta_e}{1 + (1 + \alpha_T)}} \sqrt{\frac{|\omega_{*e}|}{D_{\parallel}k_{\parallel}^2}} \frac{1 - \text{sgn}(k_y)i}{\sqrt{2}} \hat{\phi}. \quad (28)$$

We note that the phase relation is simple, since $\hat{n} \sim e^{-i\frac{\pi}{4}} \hat{\phi}$ and $\hat{T} \sim e^{-i\frac{\pi}{4}} \hat{\phi}$. Large response is expected for the density and the temperature, since $\hat{T} \sim \eta_e \hat{n} \gg \phi$. Thus we expect large response in the density and temperature field. We note that this relation raises a concern regarding probe measurements. It is often assumed that the floating potential is similar to the space or plasma potential, by assuming that the temperature fluctuations are small. This assumption does not hold for drift convective cell. This implies that care must be taken to seek for the footprint of drift convective cells in measured data.

4.3 Flux

The flux carried by the drift convective cells is calculated as

$$\begin{aligned} \frac{\Gamma_n}{n_0 c_s} &= \rho_s \left\langle \hat{n} \left(-\frac{\partial}{\partial y} \hat{\phi} \right) \right\rangle \\ &= \sum_k \frac{\rho_s |k_y|}{\sqrt{2}} |\phi_k|^2 \frac{\rho_s k_{\perp}}{\sqrt{1 + (1 + \alpha_T)\eta_e}} \sqrt{\frac{|\omega_{*e}|}{D_{\parallel}k_{\parallel}^2}}, \end{aligned} \quad (29)$$

and

$$\begin{aligned} \frac{Q_e}{T_e c_s} &= \rho_s \left\langle \hat{T} \left(-\frac{\partial}{\partial y} \hat{\phi} \right) \right\rangle \\ &= \sum_k \frac{\rho_s |k_y|}{\sqrt{2}} |\phi_k|^2 \rho_s k_{\perp} \sqrt{\frac{\eta_e}{1 + (1 + \alpha_T)}} \sqrt{\frac{|\omega_{*e}|}{D_{\parallel}k_{\parallel}^2}}. \end{aligned} \quad (30)$$

We note that both $\Gamma_n > 0$ and $Q_e > 0$. Thus drift convective cells expel both particles and heat from the system. Unlike drift waves, there is no interference of transport between density and temperature. The level of transport is expected to be large, since $\omega_{*e} \gg D_{\parallel}k_{\parallel}^2$. While these features are undesirable from confinement perspective, these feature may be useful to expand the SOL width.

5. Implications on SOL Width

The density and temperature fluctuations have different characteristics based on the electron response. Table 1 summarizes the relevant features in the adiabatic and hydrodynamic electron responses. From this, we can see that transport interference can happen in drift wave turbulence, and the inward heat pinch may occur. This can lead to a narrower SOL width, which is not desirable from the heat load handling. On the other hand, in the hydrodynamic regime, both particle and heat transport are outward, and these may result in increasing the SOL width both in the density and heat channels. In addition, a large response is expected in this regime and this feature is also beneficial for the heat load problem. In this sense, hydrodynamic, drift convective cells are thought to be benign fluctuations in the edge region.

A relevant question arises at this point: which fluctuations are excited in the experiments? To analyze this, we have performed a parameter study for several devices (Table 2). Here, we chose the parameters such that $k_{\parallel} = 1/qR$, $k_y \rho_s \sim 1$, $L_n \sim a$ and $q \sim 3$ (safety factor). The electrons drift frequency can be expressed as $\omega_{*e} = k_y \rho_s (c_s/L_n) \sim c_s/L_n = 1/a \sqrt{T_e/m_i}$. For these definitions, the key parameter is

$$\frac{\omega_{*e}}{D_{\parallel}k_{\parallel}^2} \propto \frac{(qR)^2 n_e}{a T_e^2}. \quad (31)$$

Figure 2 shows the electron density-temperature depen-

Table 1 Comparison of fluctuation characteristics.

Electrons	Adiabatic	2D, Hydrodynamic
	($D_{\parallel}k_{\parallel}^2 \gg \omega_{*e}$)	($\omega_{*e} \gg D_{\parallel}k_{\parallel}^2$)
Regime	DW	CC (linear)
Amp.	$\hat{n} \sim \hat{\phi} \gg \hat{T}$	$\hat{n} \sim \hat{T} \gg \hat{\phi}$
Phase	$\hat{n} \sim e^{-i\delta} \hat{\phi}$ $\hat{T} \sim e^{\pm i\frac{\pi}{2}} \hat{\phi}$	$\hat{n} \sim \hat{T} \sim e^{-i\frac{\pi}{4}} \hat{\phi}$
Flux	$\Gamma_n > 0$ $Q_e \rightarrow \text{both}$	$\Gamma_n > 0$ $Q_e > 0$

Table 2 Fusion device parameter.

Fusion device	Minor radius a [m]	Major radius R [m]	Ref.
C-mod	0.21	0.67	[25]
D III-D	0.67	1.7	[26]
JT-60SA	1.18	2.96	[27]
ITER	2.0	6.2	[28]

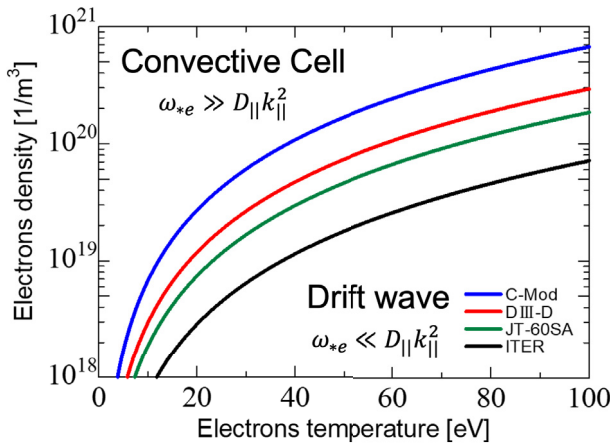


Fig. 2 Electrons density-temperature dependence of the turbulence area in each device.

dence of the turbulence domain in each fusion device. The turbulence domain is classified by the threshold $\omega_{*e}/D_{\parallel}k_{\parallel}^2 = 1$. From this, we can see that drift waves and drift convective cell may compete in the SOL. In the high-temperature and low-density SOL, the adiabatic electrons dominate and drift wave is excited. On the other hand, in the low-temperature and high-density SOL, the hydrodynamic electrons dominate and drift convective cell is excited. We also note that the boundary for the turbulence transition varies depending on machines. The parameter region for drift convective cells becomes larger for larger devices. This tendency follows from the fact that electrons need to travel longer distance along the magnetic field and hence tend to follow the hydrodynamic response. Since drift convective cells drive the outward flux both in density and temperature, this trend is favorable for the heat load reduction in future devices.

6. Conclusion and Discussion

In this paper, we discussed the excitation of drift waves and drift convective cell excited in the edge plasmas. There are two characteristic regimes exists. One is the adiabatic regimes where electrons rapidly diffuse along the magnetic field ($D_{\parallel}k_{\parallel}^2 \gg \omega_{*e}$). In this regime drift waves are excited and transport interference may occur. Electrons show different behavior when $\omega_{*e} \gg D_{\parallel}k_{\parallel}^2$. This regime is called hydrodynamic and linearly unstable convective cells

are excited. Drift convective cells transport both the particle flux and the heat flux in outward. The density and temperature response can be large and drift convective cells can effectively broaden the SOL width. The turbulence regime in the future devices are expected to be closer to the latter.

While the conclusion drawn in this work appears promising, we need further analysis for firmer basis. For simplicity, our study focuses on the behavior of main plasmas. In SOL region, however, several other physical quantities, such as neutrals [29], impurities, parallel flows, exist. We will address the effect of these degrees of freedom in future. We also note that our analysis is limited to the linear and quasilinear regimes. Nonlinear dynamics, including the excitation of secondary flows etc, will be also addressed in future.

Acknowledgments

We thank the fruitful discussion with S. Inagaki, Y. Nagashima, Y. Kawachi, K. Itoh, and participants of APTWG 2022. This work was partly supported by the Grants-in-Aid for Scientific Research of JSPS of Japan (JP18K03578, JP21H01066, JP17H06089) and by the joint research projects of RIAM, Kyushu University.

- [1] A. Loarte, B. Lipschultz, A.S. Kukushkin, G.F. Matthews, P.C. Stangeby, N. Asakura, G.F. Counsell, G. Federici, A. Kallenbach, K. Krieger, A. Mahdavi, V. Philipps, D. Reiter, J. Roth, J. Strachan, D. Whyte, R. Doerner, T. Eich, W. Fundamenski, A. Herrmann, M. Fenstermacher, P. Ghendrih, M. Groth, A. Kirschner, S. Konoshima, B. LaBombard, P. Lang, A.W. Leonard, P. Monier-Garbet, R. Neu, H. Pacher, R. Pegourie, R.A. Pitts, S. Takamura, J. Terry, E. Tsitrone and the ITPA Scrape-off Layer and Divertor Physics Topical Group, Nucl. Fusion **47**, S203 (2007).
- [2] K. Hoshino, J. Plasma Fusion Res. **92**, No.12, 882 (2016).
- [3] M.V. Umansky, T.D. Rognlien, D.D. Ryutov and P.B. Snyder, Contrib. Plasma Phys. **50**, No.3-5, 350 (2010).
- [4] P.C. Stangeby, *The Plasma Boundary of Magnetic Fusion Devices* (Institute of Physics, Bristol, 2000).
- [5] R.J. Goldston, Nucl. Fusion **52**, 013009 (2012).
- [6] X.Q. Xu, N.M. Li, Z.Y. Li, B. Chen, T.Y. Xia, T.F. Tang, B. Zhu and V.S. Chan, Nucl. Fusion **59**, 126039 (2017).
- [7] X. Garbet, C. Fenzi, H. Capes, P. Devynck and G. Antar, Phys. Plasmas **6**, 3955 (1999).
- [8] Y. Kosuga, S.-I. Itoh and K. Itoh, Contrib. Plasma Phys. **56**, No.6-8, 511 (2016).
- [9] J.R. Myra, D.A. D'Ippolito and D.A. Russell, Phys. Plasmas **22**, 042516 (2015).
- [10] Y. Kosuga, F. Kin and M. Sasaki, Contrib. Plasma Phys. **60**, e201900141 (2020).
- [11] C.S. Chang, S. Ku, A. Loarte, V. Parail, F. Köchl, M. Romanelli, R. Maingi, J.-W. Ahn, T. Gray, J. Hughes, B. LaBombard, T. Leonard, M. Makowski and J. Terry, Nucl. Fusion **57**, 116023 (2017).
- [12] N. Ohno, J. Plasma Fusion Res. **82**, No.4, 205 (2006).
- [13] S.-I. Itoh, Y. Kosuga, T. Kobayashi, M. Sasaki and K. Itoh, J. Plasma Fusion Res. **96**, No.5, 225 (2020).

- [14] X. Garbet, L. Garzotti, P. Mantica, H. Nordman, M. Valovic, H. Weisen and C. Angioni, *Phys. Rev. Lett.* **91**, 035001 (2003).
- [15] P.H. Diamond, Y. Kosuga, Ö.D. Gürçan, C.J. McDevitt, T.S. Hahn, N. Fedorczak, J.E. Rice, W.X. Wang, S. Ku, J.M. Kwon, G. Dif-Pradalier, J. Abiteboul, L. Wang, W.H. Ko, Y.J. Shi, K. Ida, W. Solomon, H. Jhang, S.S. Kim, S. Yi, S.H. Ko, Y. Sarazin, R. Singh and C.S. Chang, *Nucl. Fusion* **53**, 104019 (2013).
- [16] Y. Kosuga, S.-I. Itoh and K. Itoh, *Plasma Fusion Res.* **10**, 3401024 (2015).
- [17] S. Inagaki, T. Kobayashi, Y. Kosuga, S.-I. Itoh, T. Mitsuzono, Y. Nagashima, H. Arakawa, T. Yamada, Y. Miwa, N. Kasuya, M. Sasaki, M. Lesur, A. Fujisawa and K. Itoh, *Scientific Reports* **6**, 22189 (2016).
- [18] A. Hasegawa and M. Wakatani, *Phys. Rev. Lett.* **50**, 682 (1983).
- [19] S.I. Braginskii, *Rev. Plasma Phys.* **1**, 205 (1965).
- [20] A. Zeiler, J.F. Drake and B. Rogers, *Phys. Plasmas* **4**, 2134 (1997).
- [21] S.J. Camargo, D. Biskamp and B.D. Scott, *Phys. Plasmas* **2**, No.1, 48 (1995).
- [22] Y. Kawachi, S. Inagaki, M. Sasaki, Y. Kosuga, T. Yamada, Y. Nagashima, C. Moom, N. Kasuya and A. Fujisawa, *Plasma Fusion Res.* **16**, 1202081 (2021).
- [23] Y. Kosuga, *Phys. Plasmas* **24**, 122305 (2017).
- [24] Y. Kosuga, S.-I. Itoh and K. Itoh, *Phys. Plasmas* **24**, 032304 (2017).
- [25] I.H. Hutchinson, R. Boivin, F. Bombarda, P. Bonoli, S. Fairfax, C. Fiore, J. Goetz, S. Golovato, R. Granetz, M. Greenwald, S. Horne, A. Hubbard, J. Irby, B. LaBombard, B. Lipschultz, E. Marmor, G. McCracken, M. Porkolab, J. Rice, J. Snipes, Y. Takase, J. Terry, S. Wolfe, C. Christensen, D. Garnier, M. Graf, T. Hsu, T. Luke, M. May, A. Niemczewski, G. Tinos, J. Schachter and J. Urbahn, *Phys. Plasmas* **1**, 1511 (1994).
- [26] J.L. Luxon, *Nucl. Fusion* **42**, 614 (2002).
- [27] K. Yoshida, K. Tsuchiya, K. Kizu, H. Murakami, K. Kamiya, M. Peyrot and P. Barabaschi, *J. Plasma Fusion Res. SERIES* **9**, 214 (2010).
- [28] National Institutes for Quantum Science and Technology, <https://www.jt60sa.org/wp/>
- [29] Y. Kosuga and D. Aoki, *Plasma Phys. Control. Fusion* **62**, 105002 (2020).